Hindawi Publishing Corporation
EURASIP Journal on Advances in Signal Processing
Volume 2007, Article ID 32818, 12 pages
doi:10.1155/2007/32818

*Research Article*

# Linear Predictive Detection for Power Line Communications Impaired by Colored Noise

**Riccardo Pighi and Riccardo Raheli**

*Dipartimento di Ingegneria dell'Informazione, Università di Parma, Viale G. P. Usberti 181A, 43100 Parma, Italy*

Received 10 November 2006; Revised 21 March 2007; Accepted 13 May 2007

Recommended by Lutz Lampe

Robust detection algorithms capable of mitigating the effects of colored noise are of primary interest in communication systems operating on power line channels. In this paper, we present a sequence detection scheme based on linear prediction to be applied in single-carrier power line communications impaired by colored noise. The presence of colored noise and the need for statistical sufficiency requires the design of an optimal front-end stage, whereas the need for a low-complexity solution suggests a more practical suboptimal front-end. The performance of receivers employing both optimal and suboptimal front-ends has been assessed by means of minimum mean square prediction error (MMSPE) analysis and bit-error rate (BER) simulations. We show that the proposed optimal solution improves the BER performance with respect to conventional systems and makes the receiver more robust against colored noise. As case studies, we investigate the performance of the proposed receivers in a low-voltage (LV) power line channel limited by colored background noise and in a high-voltage (HV) power line channel limited by corona noise.



## 1. INTRODUCTION

In the last years, there has been a growing interest towards the possibility of exploiting existing power lines as effective transmission means [1, 2]. Low-voltage (LV) and medium-voltage (MV) power lines, below 1 kV and from 1 to 36 kV, respectively, are appealing because they provide a potentially convenient and inexpensive communication medium for control signaling and data communication. The structure of the distribution grid is also appropriate for internet access [3], and the existing lines can be used as backbone for local area networks or wide area networks, as a solution to the "last mile" access problem [4]. Even though power lines are an attractive solution for data transmission, a reliable high-speed communication is a great challenge due to the nature of the medium.

Communication systems over power lines have to deal with a very harsh environment [2]. Since the power grid was originally designed for electrical energy delivery rather than for data transmission, the power line medium has several less than ideal properties as a communication channel and, as a consequence, calls for communication techniques able to cope effectively with this hostile environment. The transmission medium of the power grid is characterized by a time-varying attenuation [5] and frequency selectivity [6], with possibly deep spectral notches, depending also on the location. Any transmission scheme applied to power lines has to cope with these impairments, including the intrinsic dependence of the channel model on the network topology and connected loads, the presence of high-level interference signals due to noisy loads, and the presence of colored noise. Moreover, the channel conditions can change because of connections and disconnections of inductive or capacitive loads. Finally, reflections from impedance mismatch at points where equipments are connected or from nonterminated points can result in multipath [7–9] and various types of noise [10].

High-voltage (HV) power lines, typically operating at or above 64 kV, can also be used for communication purposes, for example, in scenarios not covered by wireless or wired telecommunication infrastructures.

In low- or medium-voltage power grids, several noise sources can be found, such as, for example [11], (i) nonstationary colored thermal noise with power spectral density decreasing as the frequency increases, (ii) periodic asynchronous impulse noise related to switching operations of power supplies, (iii) periodic synchronous impulse noise mainly caused by switching actions of rectifier diodes, and

(iv) asynchronous impulse noise [12]. On the other hand, the HV power line channel is also limited by disturbances produced by events outside the transmission channel such as, for example, atmospheric phenomena, lightning [13], or disturbances originating within the system such as network switching [10], impulse noise [14–17], and corona phenomena [18–20].

In power line communications, single-carrier modulations based on quadrature amplitude modulation (QAM) or other modulation formats may be adopted for their simplicity. However, in broadband applications strong colored noise sources can severely limit the performance of single-carrier systems and demand for adequate signal processing schemes.

In this paper, we propose a single-carrier PLC scheme based on linear prediction and multidimensional coding, which exhibits good improvements, in terms of signal-to-noise ratio (SNR) necessary to achieve a given bit-error rate (BER), with respect to state-of-the-art solutions. The principle of linear predictive detectors proposed for fading channels [21–24] is a valuable and general technique that can be used every time a communication system has to cope with colored noise [25], provided that a correct statistical information on the noise is available at the receiver. First, we will introduce the linear predictive detection scheme considering a general model for the colored noise process. As case studies, we will also analyze the performance of the proposed receiver considering colored background noise for LV power lines and corona noise [19, 20] for HV power lines.

Moreover, in order to reduce the computational load of the linear predictive receiver, we apply reduced-state sequence detection techniques [26–29] such as "trellis folding by set partitioning" [30] and per-survivor processing (PSP) [29], and demonstrate the robustness of the proposed scheme in terms of BER and complexity with respect to standard solutions.

This paper expands upon preliminary work reported in [31]. With respect to [31], this paper complements the analysis comparing the BER performance of the optimal and suboptimal solutions in the presence of frequency selective LV and HV power line channels. In particular, main contributions of the article are the following:

(1) to demonstrate and compare the performance, in terms of SNR, of suboptimal and optimal front ends;
(2) for a given front end, to quantify the SNR improvements achievable by the linear predictive approach;
(3) to address the complexity of the proposed solution by means of state reduction techniques such as trellis folding by set partitioning and per-survivor processing;
(4) to extend the linear prediction algorithm to a multidimensional TCM code;
(5) to demonstrate that the linear predictive detection is an advanced signal processing technique which may be effectively applied to power line communications in order to increase the system robustness to colored noise.

The paper outline is as follows. In Section 2, we present the reduced-state multidimensional linear prediction receiver based on an optimal front end or a suboptimal practical approximation. In Section 3, we describe how linear prediction can be applied to a multidimensional observable. In Sections 4 and 5, we introduce, respectively, the channel and the colored noise models for an LV and HV power line scenarios. In Section 6, numerical results are presented. Finally, Section 7 concludes the paper.

## 2. LINEAR PREDICTION RECEIVER

Single-carrier transmission may be attractive from a complexity point of view. However, since the power line channel is affected by severe intersymbol interference (ISI) and colored noise, powerful detection and equalization techniques are necessary. Practical implementation of these schemes may also require reduced state approaches.

### 2.1. Optimal detector

Let us consider the transmission scheme depicted in Figure 1 in terms of its lowpass equivalent. We adopt a transmission system based on a four-dimensional trellis coded modulation scheme (4D-TCM) [32], which is a suitable choice to achieve high spectral efficiency and, at the same time, a good coding gain. We assume a square-root raised cosine shaping filter with frequency response $P(f)$ and a power line channel with frequency response $H(f)$, which will be detailed in Sections 4 and 5. The presence of colored noise $\eta(t)$ with power spectral density (PSD) given by $S_\eta(f)$, and the need for statistical sufficiency yield a detector front end based on a whitening filter, with frequency response $1/\sqrt{S_\eta(f)}$, and a filter matched to the overall channel response $Q^*(f)/\sqrt{S_\eta(f)}$, where $Q(f) = P(f)H(f)$, namely, a standard matched filter for colored noise [33]. The signal at the output of this filter is sampled with period equal to the signaling interval $T$. The frequency selectivity of the power line channel may be dealt with by an equalizer which limits the ISI. This equalizer can be used to reduce the amount of ISI and, as a consequence, the trellis complexity of the following sequence detector based on a Viterbi processor. As extreme cases, the equalizer may be omitted, relegating the task of dealing with ISI to the detector, or it can be very complex in order to substantially eliminate the ISI. The following derivation is general enough to encompass, as special cases, these extreme scenarios, as well as intermediate ones. After the equalizer, we use a sequence detection Viterbi processor to search an extended trellis diagram accounting for the encoder memory, the residual ISI and the channel memory induced by colored noise. This detector uses linear prediction to deal with the colored noise at its input.

As a consequence, considering the system model in Figure 1, the discrete-time observable at the input of the Viterbi processor can be expressed as

$$r_i = \underbrace{\sum_{n=0}^{L} f_n c_{i-n}}_{s_i(\mathbf{c}_{i-L}^{i})} + n_i, \tag{1}$$

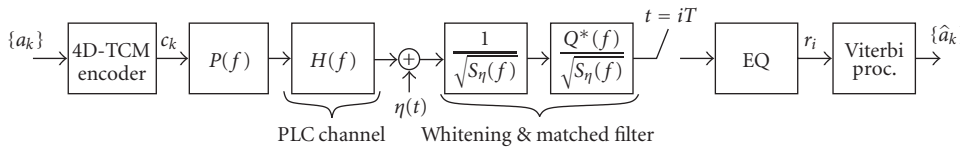


Figure 1: Simplified system model with optimum receiver for colored noise.

where[1] $f_i = g_i \otimes d_i$ denotes the overall impulse response of the system, $g_i = g(t)|_{t=iT} = p(t) \otimes h(t) \otimes m(-t)|_{t=iT}$ is the impulse response up to the output of the sampling device with $p(t) = \mathcal{F}^{-1}\{P(f)\}$, $\mathcal{F}^{-1}$ being the inverse Fourier transform operator, $h(t) = \mathcal{F}^{-1}\{H(f)\}$, $m(t) = \mathcal{F}^{-1}\{M(f)\}$ and $M(f) = Q^*(f)/S(f)$, $d_i$ is the impulse response of the equalizer, $s_i(\mathbf{c}_{i-L}^{i})$ is the noiseless signal component affected by the residual ISI of length $L$ at the output of the equalizer, $\{c_i\}$ is the code sequence with symbols belonging to a QAM constellation, and $\{n_i\}$ is a sequence of colored noise samples with PSD $S_n(e^{\jmath 2\pi f T})$. Note that the noise at the output of the matched filter $Q^*(f)/\sqrt{S_\eta(f)}$ is colored with a different PSD with respect to that associated to $\eta(t)$. Moreover, the presence of the equalizer changes also the spectral density of the noise at the input of the Viterbi processor. Finally, we assume that the colored noise can be modeled as a process with Gaussian statistics.

We now derive the optimal branch metric for a single-carrier communication scheme to be used in a sequence detection Viterbi algorithm. Collecting the samples (1) at the output of the colored noise channel into a suitable complex vector $\mathbf{r}$, we can formulate the maximum a posteriori probability (MAP) sequence detection strategy as

$$\hat{\mathbf{a}} = \arg\max_{\mathbf{a}} p(\mathbf{r} \mid \mathbf{a}) P\{\mathbf{a}\}, \tag{2}$$

where $p(\mathbf{r} \mid \mathbf{a})$ is the conditional probability density function (PDF) of the vector $\mathbf{r}$, given the data vector $\mathbf{a}$, and $P\{\mathbf{a}\}$ is the a priori probability of the information symbols. Since the trellis encoder can be described as a time-invariant finite state machine, it is possible to define a sequence of 4D states $\{\mu_0, \mu_1, \dots\}$ over which the encoder evolves and define a deterministic state transition law, function of the 4D information symbol $a_k$, which describes the evolution of the system, that is, $\mu_k = f(\mu_{k-1}, a_{k-1})$. Note that each state $\mu_k$ belongs to a set of finite cardinality. As a consequence, the evolution of the finite state machine model of the 4D-TCM encoder can be described through a trellis diagram, in which there are a fixed number of exiting branches from each state: this number will depend on the number of subsets in which the constellation is partitioned [34].

The 4D-TCM code symbol $C_k(a_k, \mu_k) = (c_{2k-1}(a_k, \mu_k), c_{2k}(a_k, \mu_k))$, with 2D components belonging to a QAM constellation, is a function of the encoder state $\mu_k$ and the information symbol $a_k$ at the input of the encoder. Note that $c_{2k-1}(a_k, \mu_k)$ and $c_{2k}(a_k, \mu_k)$ are, respectively, the first and second two-dimensional (2D) symbols transmitted over the channel during the four-dimensional time interval. Under these assumptions, we can express the 4D discrete-time observable as $R_k = (r_{2k-1}, r_{2k})$, where the 2D components are defined according to (1).

Assuming causality and finite memory [35], applying the chain factorization rule to the conditional PDF and taking into account the multidimensional structure of the TCM code, we can rewrite (2) as

$$\begin{aligned} \hat{\mathbf{a}} &= \arg\max_{\mathbf{a}} \prod_{k=0}^{K-1} p(R_k \mid \mathbf{R}_0^{k-1}, \mathbf{a}_0^{k}) P\{a_k\} \\ &\simeq \arg\max_{\mathbf{a}} \prod_{k=0}^{K-1} p(r_{2k} \mid \mathbf{r}_{2k-2-\nu}^{2k-1}, a_k, \zeta_k) \\ &\quad \cdot p(r_{2k-1} \mid \mathbf{r}_{2k-2-\nu}^{2k-2}, a_k, \zeta_k) P\{a_k\}, \end{aligned} \tag{3}$$

where $K$ is the length of the transmission and $\mathbf{r}_{k_1}^{k_2}$ is a shorthand notation for a vector collecting 2D signal observations from time epoch $k_1$ to $k_2$. In the last step of (3), in order to limit the memory of the receiver, we have assumed Markovianity of order $\nu$ in the conditional observation sequence. Moreover we define a system state accounting for the 4D-TCM coder state $\mu_k$, the order of Markovianity $\nu$, and the residual ISI span $L$ as

$$\begin{aligned} \zeta_k &= (\mu_k, C_{k-1}, C_{k-2}, C_{k-3}, \dots, C_{k-(L+\nu)/2}) \\ &= (\mu_k, c_{2k-1}, c_{2k-2}, \dots, c_{2k-\nu-L}). \end{aligned} \tag{4}$$

The assumed Markovianity results in an approximation whose quality increases with the order $\nu$.

Since we assume that the colored noise process has a Gaussian distribution, the observation is conditionally Gaussian, given the data. The application of the chain factorization rule allows us to factor the conditional PDF in (3) as a product of two complex conditional Gaussian PDFs, completely defined by the conditional means

$$\begin{aligned} \hat{r}_{2k} &= \mathbb{E}\{r_{2k} \mid \mathbf{r}_{2k-2-\nu}^{2k-1}; a_k, \zeta_k\}, \\ \hat{r}_{2k-1} &= \mathbb{E}\{r_{2k-1} \mid \mathbf{r}_{2k-2-\nu}^{2k-2}; a_k, \zeta_k\}, \end{aligned} \tag{5}$$

and the conditional variances

$$\begin{aligned} \hat{\sigma}_{r_{2k}}^2 &= \mathbb{E}\{|r_{2k} - \hat{r}_{2k}|^2 \mid \mathbf{r}_{2k-2-\nu}^{2k-1}; a_k, \zeta_k\}, \\ \hat{\sigma}_{r_{2k-1}}^2 &= \mathbb{E}\{|r_{2k-1} - \hat{r}_{2k-1}|^2 \mid \mathbf{r}_{2k-2-\nu}^{2k-2}; a_k, \zeta_k\}. \end{aligned} \tag{6}$$

[1] The operator $\otimes$ denotes convolution in continuous or discrete time.

These conditional means $\hat{r}_{2k}$ and $\hat{r}_{2k-1}$ can be interpreted as perhypothesis linear predictive estimates of $r_{2k}$ and $r_{2k-1}$, respectively; likewise, the conditional variances $\hat{\sigma}^2_{r_{2k}}$ and $\hat{\sigma}^2_{r_{2k-1}}$ are interpretable as the relevant minimum mean square prediction errors (MMSPEs) [36]. Note that, for a given value of $\nu$, the number of prediction coefficients changes with respect to the number of past samples defined in the conditioning event, that is, $\hat{r}_{2k-1}$ is evaluated using the last $\nu$ 2D observables, whereas $\hat{r}_{2k}$ is evaluated using the last $\nu+1$ 2D observables. The solution of a Wiener-Hopf matrix equation for linear prediction based on a 4D observable will be presented in Section 3.

The detection strategy (2), the factorization (3), and linear prediction allow us to derive the branch metrics to be used for joint sequence detection and decoding in a Viterbi algorithm. Taking the logarithm, assuming that the information symbols are independent and identically distributed and discarding irrelevant terms, we can express the metric of branch $(a_k, \zeta_k)$ as

$$\lambda_k(a_k,\zeta_k) \propto \sum_{i=0}^{1} \ln p\left(r_{2k-i} \mid \mathbf{r}_{2k-2-\nu}^{2k-1-i}; a_k, \zeta_k\right), \tag{7}$$

where the symbol $\propto$ denotes a monotonic relation with respect to the variable of interest (i.e., the data sequence). The detection strategy (2) can be now formalized as

$$\hat{\mathbf{a}} = \arg\min_{\mathbf{a}} \sum_{k=0}^{K-1} \lambda_k(a_k,\zeta_k), \tag{8}$$

where the branch metrics are expressed as

$$\lambda_k(a_k,\zeta_k) = \sum_{i=0}^{1} \left\{ \frac{\left| r_{2k-i} - \hat{r}_{2k-i} \right|^2}{\hat{\sigma}^2_{r_{2k-i}}} + \ln \hat{\sigma}^2_{r_{2k-i}} \right\}. \tag{9}$$

Finally, the state complexity of a linear predictive receiver can be limited by means of state-reduction techniques [26–29]. Let $S = S_c M^{(\nu+L)/2}$ denote the state complexity of the proposed receiver, where $S_c$ is the number of states of the 4D-TCM encoder, $M$ is the cardinality of the 2D constellation, and $Q < (\nu+L)/2+1$ denotes the memory parameter taken into account in the definition of a "reduced" trellis state

$$\omega_k = \left(\mu_k, I_{k-1}(1), I_{k-2}(2), \ldots, I_{k-Q}(Q)\right) \tag{10}$$

in which, for $i = 1,\ldots,Q$, $I_{k-i}(i) \in \Omega(i)$ are subsets of the code constellation and $\Omega(i)$ are partitions of the code constellation.[2] Defining $J_i = \mathrm{card}\{\Omega(i)\}$, $i = 1,\ldots,Q$ as the cardinality of the partition $\Omega(i)$, the number of reduced-states in the trellis diagram can be expressed as [26, 28]

$$S' = S_c \prod_{i=1}^{Q} \frac{J_i}{2}. \tag{11}$$

[2] $C_{k-i} \in \Omega(i)$ are 4D-coded symbols compatible with the given state.

The branch metric can be obtained by defining a "pseudo state" [30]

$$\tilde{\zeta}_k(\omega_k) = \Bigg( \underbrace{\mu_k, \widetilde{C}_{k-1}(\omega_k), \ldots, \widetilde{C}_{k-Q}(\omega_k)}_{Q+1 \text{ elements}}, \underbrace{\check{C}_{k-Q-1}(\omega_k), \ldots, \check{C}_{k-Q-P}(\omega_k)}_{P \text{ code symbols}} \Bigg), \tag{12}$$

where $\widetilde{C}_{k-1}(\omega_k),\ldots,\widetilde{C}_{k-Q}(\omega_k)$ are $Q$ code symbols compatible with state $\omega_k$ to be found in the survivor history of state $\omega_k$, and $P$ are code symbols chosen by a per-survivor processing (PSP) technique [29], that is, $\check{C}_{k-Q-1}(\omega_k),\ldots,\check{C}_{k-Q-P}(\omega_k)$ are the $P$ 4D-TCM code symbols associated with the survivor of $\omega_k$. The branch metric $\widetilde{\lambda}_k(I_k(1),\omega_k)$ in the reduced-state trellis can be defined in terms of the pseudostate (12) according to

$$\widetilde{\lambda}_k(I_k(1),\omega_k) = \min_{C_k \in I_k(1)} \lambda_k\left(a_k, \widetilde{\zeta}_k(\omega_k)\right) \tag{13}$$

assuming that the pseudo state $\widetilde{\zeta}_k(\omega_k)$ is compatible with $\omega_k$, that is, $C_{k-i} \in I_{k-i}(i)$.

As already noted in Section 2.1, we point out the fact that the formulation of the reduced-state linear predictive approach detailed in this article is general and its validity is independent from the ISI-removing capacity of the equalizer. In particular, if the equalizer is ideal, $L$ should be set to zero; if a realistic equalizer is used, some residual ISI may be present and can be duly accounted for by a proper selection of $L$. Finally, if the equalizer is absent, it is still possible to encompass the ISI using a joint sequence detection and decoding approach. In conclusion, the proposed approach may be applied to every kind of equalization scheme. In the absence of explicit knowledge of the amount of residual ISI, it is possible to select a sufficiently large value for $L$. However, since the parameter $L$ affects the complexity of the Viterbi processor, the selected value should be kept as small as possible in order to limit the implementation cost.

### 2.2. Suboptimal detector

Since the optimal front end may be quite complex from a practical point of view, requiring adaptivity and high-computational load during the filtering process, in Figure 2, a suboptimal, more practical alternative is also presented. Instead of performing the whitening operation in the analog front-end stage, we propose a linear predictive receiver in which signal processing, necessary for coping with the colored noise, is entirely done in a digital fashion, that is, modifying the branch metric of a Viterbi processor. The shaping and receiver filter can be both selected with square-root raised cosine frequency response, so that noise samples are white when the overall noise process is white. Since the signal processing associated to the suboptimal front end is different from the processing done by the optimal front end, the PSD of the colored noise at the input of the Viterbi processor is different. Moreover, we still assume that the equalizer

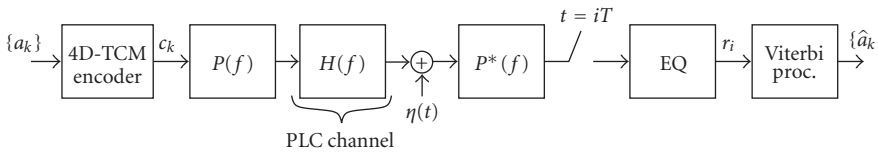


Figure 2: Simplified system model with a suboptimal implementation of the front-end filter.

may leave some residual ISI into the signal at the input of the Viterbi processor: under this assumption, the discrete time observable $r_i$ may be defined as in (1), with a different impulse response $f_i$ and noise spectrum.

The proposed suboptimal front end may be used to upgrade a PLC system, originally not designed for a scenario limited by colored noise, by simply modifying the Viterbi processor while leaving unchanged the, possibly analog, front-end stage. As previously outlined, the Viterbi processor enables sequence detection and decoding, searching an extended trellis diagram including the residual ISI and the code memory, using a branch metric defined as in (9) and possibly state-reduction techniques as presented in (12) and (13).

Finally, note that the proposed suboptimal solution with linear prediction may be an effective approach for communication systems which have to deal with time-varying channel conditions, simplifying the adaptivity of the receiver. In particular, it is possible to recursively adapt the values of the prediction coefficients by applying standard techniques, like those based on stochastic gradient algorithms [36].

## 3. MULTIDIMENSIONAL LINEAR PREDICTION

In this section, we describe how linear prediction can be applied to a 4D observation vector collecting $R_k$ and how to obtain an estimate of the colored noise samples at the output of the matched filter. We start defining a cost function $J$ which represents the conditional mean square error between the colored noise samples and a possible set of estimates of the noise process.

It is possible to express the cost function as[3]

$$J(\mathbf{P}) = \mathbb{E}\left\{\left\| \left[R_k - S_k(\mathbf{C}_{k-L/2}^{k})\right] - \sum_{i}^{\nu/2} \mathbf{P}_i \left[\mathbf{R}_{k-i} - \mathbf{S}_{k-i}(\mathbf{C}_{k-i-L/2}^{k-i})\right] \right\|^2 \mid a_k, \zeta_k \right\}, \tag{14}$$

where $\mathbf{P}$ is a matrix collecting all prediction coefficients, $S_k(\mathbf{C}_{k-L/2}^{k})$ is the noiseless 4D signal component affected by ISI and $\|\cdot\|^2$ is the Euclidean norm. The quantity $R_k - S_k(\mathbf{C}_{k-L/2}^{k})$ represents the colored noise sample we wish to predict on the correct trellis path. Similarly, the quantities $\{\mathbf{R}_{k-i} - \mathbf{S}_{k-i}(\mathbf{C}_{k-i-L/2}^{k-i})\}_i^{\nu/2}$ are related to the *data* [36], that is, the per-survivor past samples of colored noise, to be used to perform linear prediction.

The cost function (14) can be expressed explicitly as

$$\begin{aligned} J(\mathbf{P}) = \mathbb{E}\Bigg\{ & \left| \left[r_{2k-1} - s_{2k-1}(\mathbf{c}_{2k-1-L}^{2k-1})\right] - \sum_{i=1}^{\nu} p_{1,i}\left[r_{2k-1-i} - s_{2k-1-i}(\mathbf{c}_{2k-1-i-L}^{2k-1-i})\right] \right|^2 \\ & + \left| \left[r_{2k} - s_{2k}(\mathbf{c}_{2k-L}^{2k})\right] - \sum_{i=0}^{\nu} p_{2,i}\left[r_{2k-1-i} - s_{2k-1-i}(\mathbf{c}_{2k-1-i-L}^{2k-1-i})\right] \right|^2 \mid a_k, \zeta_k \Bigg\}. \end{aligned} \tag{15}$$

Since the cost function is a sum of two positive functions of disjoint sets of variables, that is, $J(\mathbf{P}) = J_1(\mathbf{p}_1) + J_2(\mathbf{p}_2)$ with $\mathbf{p}_1$ and $\mathbf{p}_2$, respectively, the prediction vectors for the first and second 2D observable, the minimization can be performed separately on each function. In the following, we show how to obtain the prediction coefficients for the first 2D component of the 4D observable (i.e., $\{p_{1,i}\}$). Defining *data* vectors

$$\mathbf{d}_{2k-2-\nu}^{2k-2} = \left(\mathbf{r}_{2k-2-\nu}^{2k-2} - \mathbf{s}_{2k-2-\nu}^{2k-2}(\mathbf{c}_{2k-2-\nu-L}^{2k-2})\right)^T \tag{16}$$

collecting $\nu$ per-survivor noise samples at the input of the Viterbi processor, we can express the cost function as[4]

$$J_1(\mathbf{p}_1) = \mathbb{E}\left\{\left[d_{2k-1} - \mathbf{p}_1^T \cdot \mathbf{d}_{2k-2-\nu}^{2k-2}\right] \cdot \left[d_{2k-1} - (\mathbf{p}_1^T \cdot \mathbf{d}_{2k-2-\nu}^{2k-2})^H\right] \mid a_k, \zeta_k \right\}. \tag{17}$$

Taking the gradient with respect to the prediction vector $\mathbf{p}_1$ we are now able to formulate the Wiener-Hopf equation as

$$\mathbf{R}_\nu \cdot \mathbf{p}_1 = \mathbf{q}_\nu, \tag{18}$$

where the system matrix, with dimension $\nu \times \nu$, is defined as

$$\mathbf{R}_\nu = \mathbb{E}\left\{[\mathbf{d}_{2k-2-\nu}^{2k-2}] \cdot [\mathbf{d}_{2k-2-\nu}^{2k-2}]^H \mid a_k, \zeta_k \right\} \tag{19}$$

[3] For notational simplicity, we omit the dependence of the code symbol on the state $\zeta_k$ and input symbols $a_k$, that is, $C_k$ is used in place of $C_k(a_k, \zeta_k)$.

[4] Superscripts $T$ and $H$ denote transpose and Hermitian transpose operators, respectively.

and the vector of $\nu$ known terms is

$$\mathbf{q}_\nu = \mathbb{E}\{d_{2k-1}\mathbf{d}_{2k-2-\nu}^{2k-2} \mid a_k, \zeta_k\}. \tag{20}$$

We remark that the per-survivor noise samples $\mathbf{d}_{2k-2-\nu}^{2k-2}$ are not available at the detector: they must be evaluated through the observation of the output of the front end and a reconstruction of noiseless signal components associated with the survivor path leading to state $\zeta_k$.

The linear system defined in (18) can now be solved using Cholesky factorization [36], obtaining the prediction coefficient vector

$$\mathbf{p}_1 = \mathbf{R}_\nu^{-1} \cdot \mathbf{q}_\nu. \tag{21}$$

As to the second 2D observable, the prediction coefficients $\{p_{2,i}\}$ and the cost function $J_2(\mathbf{p}_2)$ can be determined in a similar manner, noting that in the evaluation of the estimate $\mathbb{E}\{r_{2k} \mid \mathbf{r}_{2k-2-\nu}^{2k-1}; a_k, \zeta_k\}$ we can also use the observable at time $2k-1$ from the most recent previous 2D observable.

Finally, rewriting the cost functions $J_1(\mathbf{p}_1)$ and $J_2(\mathbf{p}_2)$ as explicit functions of the predictor vectors $\mathbf{p}_1$ and $\mathbf{p}_2$, respectively, we can express the minimum mean square prediction errors as

$$\begin{aligned} J_1(\mathbf{p}_1) &= \sigma_n^2 - \mathbf{p}_1^T \cdot \mathbf{q}_\nu \\ J_2(\mathbf{p}_2) &= \sigma_n^2 - \mathbf{p}_2^T \cdot \mathbf{q}_{\nu+1}, \end{aligned} \tag{22}$$

where $\sigma_n^2$ is the colored noise power at the input of the Viterbi processor.

## 4. LOW- AND MEDIUM-VOLTAGE POWER LINE CHANNEL

### 4.1. Colored noise model

Besides frequency selectivity, the dominant channel disturbances occurring in power line channels in the frequency range between a few hundred kHz and 20 MHz are colored background noise, narrowband interference and impulse noise. Some measurements at high frequencies have been reported in [37, 38]. In this work, we represent the colored PSD using a simple three-parameter model presented in [39], that is,[5]

$$S_{\eta c}(f) = a + b \cdot |f|^c \frac{\text{dBm}}{\text{Hz}} \tag{23}$$

with $a = -145$, $b = 53.23$ and $c = -0.337$. Despite the fact that a realistic PSD may present some variations with respect to the PSD predicted by (23), this simple model allows us to capture the main characteristic of the colored background noise, that is, the fact that the PSD decreases as the frequency increases.

Note that (23) defines a power spectrum whose frequency components are over the entire frequency domain, that is, its bandwidth is generally greater than that used by the transmission system. In our simulation, we derive an equivalent complex lowpass filtered version of the colored background noise process within the bandwidth of the considered signaling scheme. The filter used for the generation of colored noise is a finite impulse response (FIR) complex filter with coefficients obtained using Cholesky factorization [36] applied to the complex lowpass filtered colored noise power spectrum.

Finally, it should be pointed out that the noise in power lines may be modeled as nonstationary [40]. In this work, we assume that the changes in the noise PSD are slow enough to allow a correct estimation of the prediction coefficients.

### 4.2. Channel model

LV power line channels have a tree-like topology with branches formed by additional wires connected to the main path, having different length and different load impedence. The channel exhibits notches due to reflections caused by impedence mismatches. Several approaches for modeling the transfer function of LV power lines can be found in the literature. Probably, the most widely known model for the channel frequency response $H_c(f)$ of LV and MV PLC channels is the multipath model proposed by Philipps [7] and Zimmermann and Dostert [8]. Following this model, the frequency response of the channel may be expressed, in the frequency range from 500 kHz to 20 MHz, as[6]

$$H_c(f) = \sum_{i=1}^{N} g_i e^{-(a_0 + a_1 f^k)d_i} e^{-j2\pi f d_i / v_p}, \tag{24}$$

where $N$ is the number of relevant propagation paths, $a_0$ and $a_1$ are link attenuation parameters, $k$ is an exponent with typical values ranging from 0.5 to 1, $g_i$ is the weighting factor for path $i$, $d_i$ is the length of the $i$th path, and $v_p$ is the phase velocity. In this work we consider a PLC channel modeled by (24) with parameters [8] $a_0 = 0$, $a_1 = 8.10^{-6}$, $k = 0.5$, $N = 4$, $\{g_i\}_{i=1}^4 = \{0.4, -0.4, -0.8, -1.5\}$, and $\{d_i\}_{i=1}^4 = \{150, 188, 264, 397\}$. In Figure 3 the LV power line channel amplitude response based on these parameter values along with an idealized spectrum used by the systems considered in our simulations are shown.

## 5. HIGH-VOLTAGE POWER LINE CHANNEL

### 5.1. Corona noise model

The PLC channel may consist of one or more conductors, depending on the considered coupling scheme, that is, phase-to ground or phase to phase [41]. Corona noise is a common noise source for HV transmission lines, since it is permanent and its intensity depends on (i) the service voltage, (ii) the geometric configuration of the power line, (iii) the type of

[5] Note that $S_\eta(f)$ in Figures 1 and 2 is the lowpass equivalent PSD of $S_{\eta c}(f)$ with respect to the carrier frequency.

[6] Note that $H(f)$ in Figures 1 and 2 is the lowpass equivalent of $H_c(f)$ with respect to the carrier frequency.

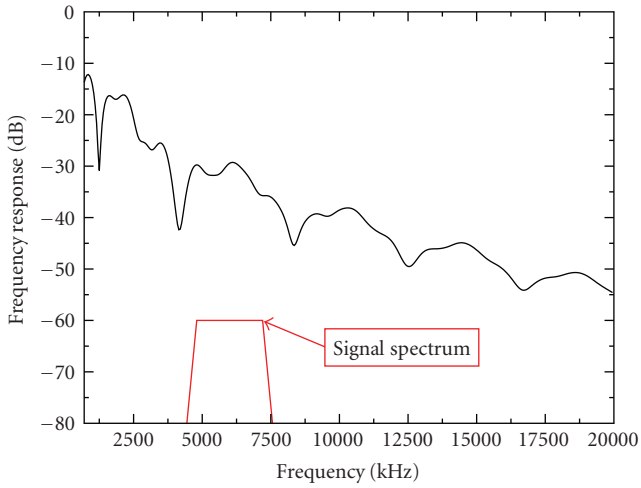


FIGURE 3: Frequency response of the simulated LV power line channel and the transmission spectrum used by the considered single-carrier PLC system.

conductors involved in the line and (iv) the atmospheric conditions.

Corona noise is caused by partial discharges on insulators and in air surrounding electrical conductors of power lines [42]. When HV power lines are in operation, the voltage originates a strong electric field in the vicinity of the conductor. This electric field accelerates free electrons present in the air nearby conductors: these electrons collide with molecules of the air, generating a free electron and positive ion couple. This process continues forming an avalanche phenomenon called "corona discharge." The motion of positive and negative charges induces a current both in the conductors and ground [18].

The induced current appears like a train of current pulses, with random pulse amplitude variations and random interarrival intervals. The injected current due to corona noise on one conductor can be modeled by a current source [18, 42]: according to Shockley-Ramo theorem [41], a corona discharge induces current in all conductors, that is, each conductor of the power line channel is connected to the ground by a current source.

A few corona noise models are present in the literature [13, 18–20]: in this article, the model proposed in [19, 20] is considered. Corona noise, as a random signal, is characterized equivalently through its autocorrelation function or its power spectrum. To this purpose, the corona noise spectrum is generated by a method that takes into account the generation phenomena of corona currents injected in the conductors and the propagation along the line [43, 44]. This spectrum is utilized to synthesize an autoregressive (AR) digital filter [36], whose output is described by the expression

$$n_k = \sum_{\ell=1}^{N} v_\ell n_{k-\ell} + w_k, \tag{25}$$

where $\{w_k\}$ is a sequence of independent zero-mean Gaussian random variables and $\{v_\ell\}_{\ell=1}^{N}$ is the set of coefficients

TABLE 1: Values of the digital filter coefficients $\{v_\ell\}_{\ell=1}^{4}$ in (25) for various service voltages.

| Voltage [kV] | $v_1$ | $v_2$ | $v_3$ | $v_4$ |
|---|---|---|---|---|
| 225 | −1.225 | 1.052 | −0.603 | 0.217 |
| 380 | −1.298 | 1.109 | −0.625 | 0.210 |
| 750 | −1.302 | 1.041 | −0.611 | 0.207 |
| 1050 | −1.292 | 1.080 | −0.647 | 0.224 |

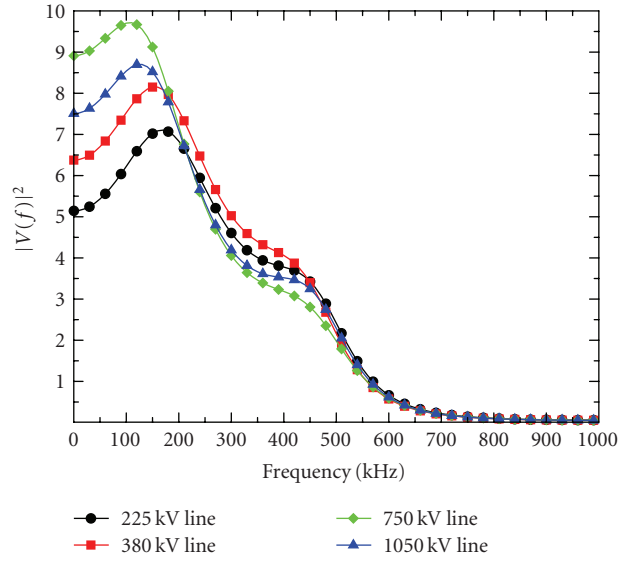


FIGURE 4: Corona noise power spectrum, shown in terms of the frequency response $V(f)$ of the AR filter in (25).

modeling the corona noise process. The synthesis of the digital filter essentially calls for the identification of the coefficients $\{v_\ell\}_{\ell=1}^{N}$ and can be done using a procedure based on the maximum entropy method proposed in [45] or on the minimization of the difference between estimated and measured power spectra.

Table 1 shows, for $N = 4$, a complete set of coefficients modeling the corona noise for different voltage lines with carrier couplings of lateral phase-to-ground type [20].

Note that, as already outlined, (25) defines a corona power spectrum whose frequency components are over the entire frequency domain, that is, its bandwidth is generally greater than that used by the transmission system. As a consequence, we derive an equivalent lowpass-filtered complex version of the corona noise process within the bandwidth of the considered signaling scheme. In Figure 4, the corona noise power spectrum obtained with the model presented in (25) with coefficients shown in Table 1 is also presented in terms of the power frequency response $|V(f)|^2$ of the AR digital filter.

### 5.2. Channel model

In this section, we describe the model used for an HV power line channel. Since the transfer function of HV power lines

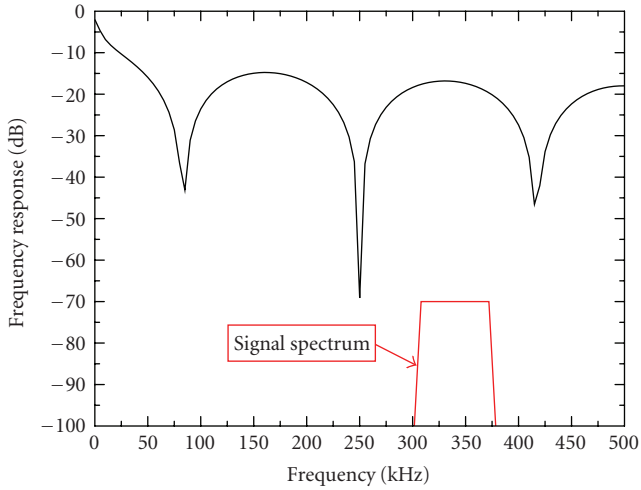


Figure 5: Frequency response of the considered 225 kV power line channel and the transmission spectrum used by the single-carrier PLC system.

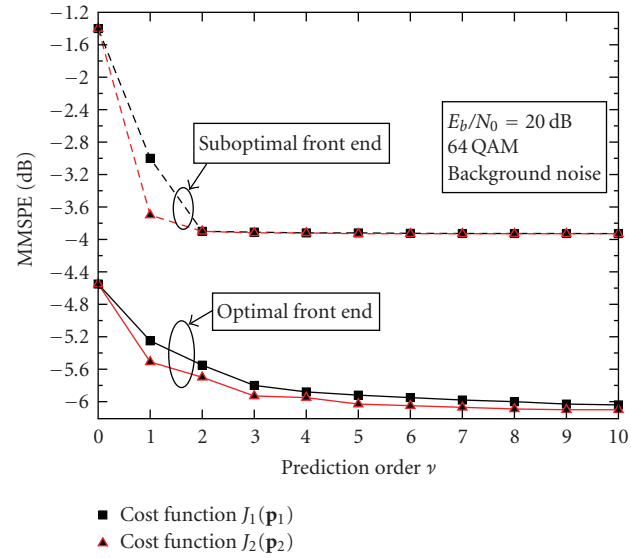


Figure 6: MMSPEs, normalized to the power of the signal $s_i(\mathbf{c}_{i-L}^i)$, as a function of the prediction order $\nu$, assuming a 64 QAM constellation, signaling frequency $f_s = 2.4$ MHz, and carrier frequency $f_c = 6$ MHz.

exhibits a strong dependence on the operating atmospheric conditions and on the different kind of loads connected to the line, a universally accepted model for the impulse response of the channel has still not been formulated. As a consequence, in this work we have used a simple HV channel model as similar as possible to a realistic scenario, including the most important limiting characteristics, that is, frequency selectivity and high attenuation.

Figure 5 shows the transfer function $H_c(f)$ used in our simulation to model a 225 kV channel along with an idealized spectrum used by the systems considered in our simulations. Note that, due to the lowpass frequency response of the coupling devices and regulatory standards, the transmission bandwidth for HV power line communications is limited to a range from 100 to 500 kHz.

## 6. NUMERICAL RESULTS

In this section, we provide the numerical results obtained applying the proposed reduced-state linear predictive solutions to two different scenarios. First, we compare the performance of a single-carrier transmission system operating on an LV power line channel affected by colored background noise using the optimal and suboptimal front ends. Then we consider the performance of a single-carrier transmission system working on an HV power line channel impaired by corona noise, using either the optimal or the suboptimal front end. The SNR is defined at the input of the receiver as $E_b/N_0$, where $E_b$ is the received energy per information bit and $N_0$ is defined as the average equivalent white noise intensity which yields the total noise power in the transmission bandwidth $B$ at the input of the receiver

$$N_0 = \frac{1}{B}\int_B S_\eta(f)df. \tag{26}$$

Since the main focus of this paper is on linear predictive detection for colored noise, we assume that the equalizer shown in Figures 1 and 2 is an ideal zero-forcing equalizer able to completely remove the ISI introduced by the channel ($L = 0$). As a consequence, the discrete-time signal at the input of the Viterbi processor can be modeled according to (1) with $L = 0$.

Finally, note that the stationarity assumption for the channel and noise is acceptable for LV PLC because the signaling frequency $f_s$ is much larger than the main frequency. As to HV PLC, the main source of colored noise, that is, the corona noise, presents a quasistationary nature with a rate of change that is orders of magnitude lower than the signaling frequency $f_s$, that is, its variation is very slow compared with the signaling period used by the PLC system. As a consequence, the assumption of stationarity for the corona noise is also very reasonable.

### 6.1. Low-voltage channel: MMSPE analysis

Let us consider first a single-carrier PLC system operating on an LV power line with frequency response defined as in Section 4.2. We adopt a transmission system based on an 8-state 4D-TCM code applied to a 64 QAM constellation, a square root raised cosine pulse as shaping filter with a roll-off factor $\alpha$ equal to 0.3, a signaling and carrier frequencies equal to, respectively, $f_s = 2.4$ MHz and $f_c = 6$ MHz.

In Figure 6, the performance of the linear predictor is assessed in terms of MMSPEs versus the prediction order $\nu$ for a fixed $E_b/N_0$ of 20 dB. In this figure the MMSPE has been normalized to the power of the useful signal $s_i(\mathbf{c}_{i-L}^i)$. The colored background noise process is generated according to the model presented in Section 4.1. We show the cost function

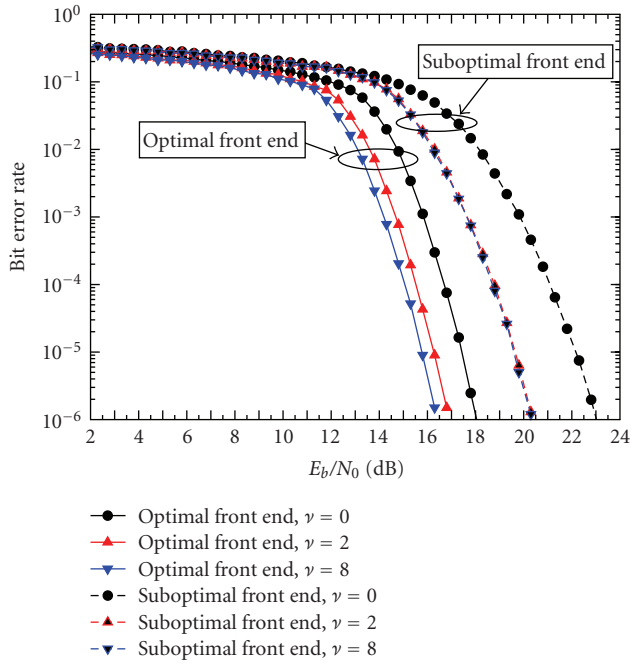


FIGURE 7: Performance of the proposed receivers for 4D-TCM 64 QAM and various values of prediction order, obtained with an 8-state 4D-TCM code applied to a 64 QAM constellation, signaling frequency $f_s = 2.4$ MHz and carrier frequency $f_c = 6$ MHz. The LV power line channel is modeled as in Section 4.2.

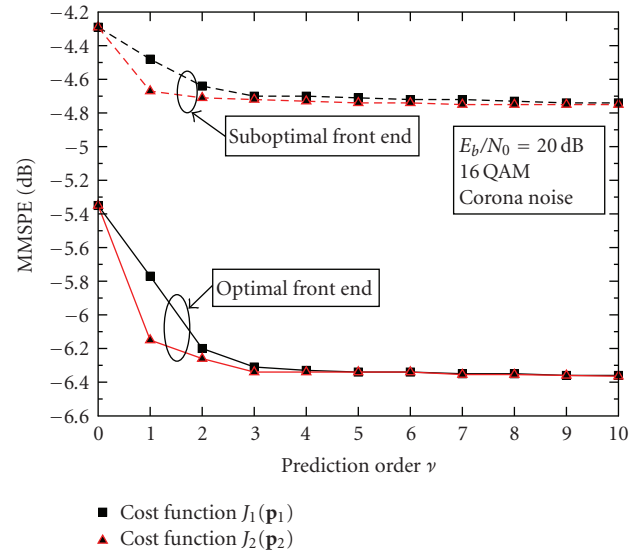


FIGURE 8: MMSPEs, normalized to the power of the signal $s_i(\mathbf{c}_{i-L}^i)$, as a function of the prediction order $\nu$, assuming a 64 QAM constellation, signaling frequency $f_s = 64$ kHz, and carrier frequency $f_c = 340$ kHz.

$J_1(\mathbf{p}_1)$ related to the estimate of the first 2D observable and the cost function $J_2(\mathbf{p}_2)$ related to the second 2D observable. Note that the prediction order $\nu$ is expressed in terms of signaling intervals, that is, $\nu = 2$ means that two 2D observables are needed for the computation of $\hat{r}_{2k-1}$ and three 2D observables are used for the computation of $\hat{r}_{2k}$. The continuous lines in Figure 6 show the normalized MMSPE performance achievable using the optimal front end, while the dashed lines present the MMSPE gain obtained using the suboptimal front end. Assuming a prediction order $\nu = 8$, the MMSPE gain shown in Figure 6 is 1.8 dB for the optimal receiver and 2.4 dB for the suboptimal receiver.

### 6.2. Low-voltage channel: BER analysis

Continuous lines (curves with labels "optimal front end") and dashed line (curves with labels "suboptimal front end") in Figure 7 show, respectively, the BER performance, in the presence of colored noise, of a single-carrier PLC system employing the proposed optimal and suboptimal front ends. We assume that the communication system is based on the same parameters used in the derivation of the MMSPE analysis described in Section 6.1. The 4D-TCM code rate allows an achievable bit rate equal to 13.2 Mbit/s. The PLC system operates over an LV power line channel with frequency response defined as in Section 4.2.

In Figure 7, the BER performance of this PLC system without linear prediction and the improvements, in terms of $E_b/N_0$, obtainable using the linear predictive receiver with both types of front ends are also shown. The BER curves in Figure 7 were obtained using different values of the prediction order $\nu$, a reduced state defined as $\omega_k = (\mu_k, I_{k-1}(1))$, that is, $Q = 1$ with $J_1 = 8$, and extracting the past $\nu$ 2D code symbols using PSP ($P$ equal to half the prediction order $\nu$). The curves obtained without linear prediction ("optimal front end, $\nu = 0$" and "suboptimal front end, $\nu = 0$" curves) show the performance of a single-carrier system which operates with a trellis complexity of $S = S_c = 8$. The used set of state reduction parameters allows the Viterbi processor to search a trellis diagram, according to (11), with a reduced number of states equal to $S' = 32$. Note that the achievable SNR gains associated to the optimal and suboptimal receiver front ends are in good agreement with the numerical MMSPE analysis presented in Figure 6.

From Figure 7 one can also observe that, for a given prediction order $\nu$, the gain, in terms of $E_b/N_0$ at BER value of $10^{-6}$, achievable using a receiver based on the optimal front-end is approximately 4 dB with respect to the suboptimal solution.

### 6.3. High-voltage channel: MMSPE analysis

We also consider a PLC system working on an HV power line. The channel is modeled as described in Section 5.2. The corona noise process is generated according to the model for a 225 kV line in Table 1 with carrier frequency centered at $f_c = 340$ kHz. The communication system employs a 4D-TCM code applied to a 16 QAM constellation, a roll-off factor $\alpha = 0.2$, and a signaling frequency $f_s = 64$ kHz.

In Figure 8 the performance of the linear predictor is assessed in terms of normalized MMSPEs versus the prediction order $\nu$ for a fixed $E_b/N_0$ of 12 dB. The continuous lines in

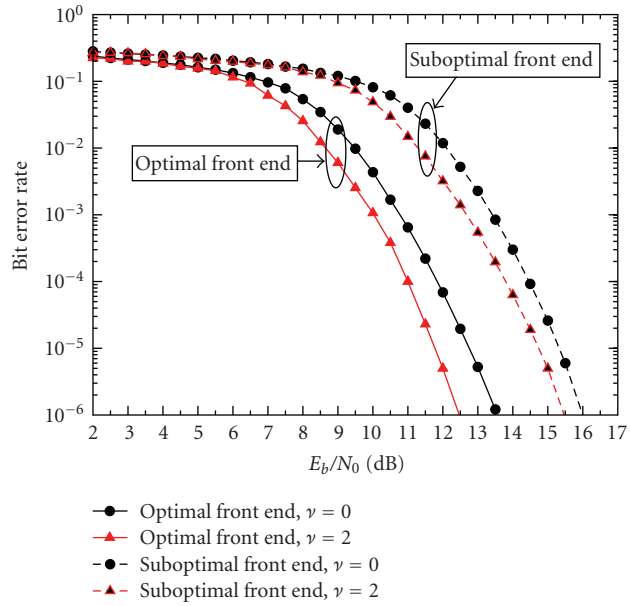


Figure 9: Performance of the proposed receivers for 4D-TCM 16 QAM and different prediction order, obtained with an 8-state 4D-TCM code applied to a 16 QAM constellation, signaling frequency $f_s = 64$ kHz, and carrier frequency $f_c = 340$ kHz. The HV power line channel is modeled as in Section 5.2.

Figure 8 show the MMSPE performance achievable using the optimal front-end, while the dashed lines present the MMSPE gain obtained using the suboptimal front end. The gain shown in Figure 8 is, for the optimal receiver, approximately 1 dB, while for the suboptimal receiver, it is about 0.4 dB. These results can be interpreted noting that the length of the corona noise correlation sequence is shorter than that of the background colored noise used in the LV system: as a consequence, the linear predictive approach operates on a less significant characterization of the noise, allowing to achieve low MMSPE gains with respect to those previously derived in the LV system, that is, compared with the MMSPE gain presented in Figure 6.

### 6.4. High-voltage channel: BER analysis

The system considered in the previous section has also been assessed in terms of BER performance. In Figure 9, continuous lines show the BER performance, in the presence of corona noise, for the same PLC system used in Section 6.3 to obtain the MMSPE analysis, corresponding to a bit rate equal to 224 kbit/s.

The BER curves in Figure 9 with linear prediction were obtained using a reduced state defined as $\omega_k = \mu_k$, that is, including only the state of the TCM coder ($Q = 0$), and extracting the past $\nu/2$ 4D-TCM code symbols using a PSP approach ($P$ equal to half the prediction order $\nu$). This set of state parameters allows one to implement a Viterbi algorithm, according to (11), with a number of reduced states equal to $S' = 8$, that is, a trellis complexity equal to that associated with a receiver operating without linear prediction.

For a target BER of $10^{-6}$, the $E_b/N_0$ gain exhibited by the system employing the optimal front end and linear prediction ($\nu = 2$), with respect to a single-carrier PLC system without linear prediction ($\nu = 0$), is approximately 1 dB. As to the suboptimal solution, the $E_b/N_0$ gain is about 0.5 dB. Moreover, the optimal receiver outperforms the suboptimal one with an SNR gain, at BER of $10^{-6}$, equal approximately to 3 dB.

## 7. CONCLUSIONS

In this paper, receivers with optimal and suboptimal front ends based on linear prediction and reduced-state sequence detection applied to single-carrier PLC system operating on channels impaired by colored Gaussian noise have been presented. The optimal branch metric to be used in a sequence detection Viterbi algorithm has been derived, along with an extension of linear prediction to a multidimensional observable. As case studies, the proposed receiver was shown to be effectively applicable to an LV PLC channel limited by colored background noise and an HV PLC channel limited by corona noise. Numerical results, assessed by means of MMSPE analysis and BER simulations, have confirmed that the proposed solutions may be able to improve the $E_b/N_0$ performance of a conventional single-carrier PLC system by approximately 1.5 dB for the LV optimal receiver limited by colored noise and 1.0 dB for the HV optimal detector impaired by corona noise.

## ACKNOWLEDGMENT

Part of this work was presented at the IEEE International Symposium on Power Line Communications, ISPLC'06, Orlando, Florida, USA, March 2006.

## REFERENCES

[1] H. C. Ferreira, H. M. Grove, O. Hooijen, and A. J. H. Vinck, "Power line communications: an overview," in *Proceedings of the 4th IEEE AFRICON Conference*, vol. 2, pp. 558–563, Stellenbosch, South Africa, September 1996.

[2] E. Biglieri, "Coding and modulation for a horrible channel," *IEEE Communications Magazine*, vol. 41, no. 5, pp. 92–98, 2003.

[3] S. Galli, A. Scaglione, and K. Dostert, "Broadband is power: internet access through the power line network," *IEEE Communications Magazine*, vol. 41, no. 5, pp. 82–83, 2003.

[4] W. Liu, H. Widmer, and P. Raffin, "Broadband PLC access systems and field deployment in European power line networks," *IEEE Communications Magazine*, vol. 41, no. 5, pp. 114–118, 2003.

[5] S. Barmada, A. Musolino, and M. Raugi, "Innovative model for time-varying power line communication channel response evaluation," *IEEE Journal on Selected Areas in Communications*, vol. 24, no. 7, pp. 1317–1326, 2006.

[6] S. Galli and T. C. Banwell, "A deterministic frequency-domain model for the indoor power line transfer function," *IEEE Journal on Selected Areas in Communications*, vol. 24, no. 7, pp. 1304–1316, 2006.

[7] H. Philipps, "Modelling of power line communication channels," in *Proceedings of the 3rd International Symposium on Power-Line Communications and Its Applications (ISPLC '99)*, pp. 14–21, Lancaster, UK, March-April 1999.

[8] M. Zimmermann and K. Dostert, "A multipath model for the power line channel," *IEEE Transactions on Communications*, vol. 50, no. 4, pp. 553–559, 2002.

[9] P. Amirshahi and M. Kavehrad, "High-frequency characteristics of overhead multiconductor power lines for broadband communications," *IEEE Journal on Selected Areas in Communications*, vol. 24, no. 7, pp. 1292–1303, 2006.

[10] H. Meng, Y. L. Guan, and S. Chen, "Modeling and analysis of noise effects on broadband power line communications," *IEEE Transactions on Power Delivery*, vol. 20, no. 2, part 1, pp. 630–637, 2005.

[11] M. Götz, M. Rapp, and K. Dostert, "Power line channel characteristics and their effect on communication system design," *IEEE Communications Magazine*, vol. 42, no. 4, pp. 78–86, 2004.

[12] V. Degardin, M. Lienard, A. Zeddam, F. Gauthier, and P. Degauque, "Classification and characterization of impulsive noise on indoor power line used for data communications," *IEEE Transactions on Consumer Electronics*, vol. 48, no. 4, pp. 913–918, 2002.

[13] A. Mujčić, N. Suljanović, M. Zajc, and J. F. Tasič, "Power line noise model appropriate for investigation if channel coding methods," in *Proceedings of the International Conference on Computer as a Tool (EUROCON '03)*, vol. 1, pp. 299–303, Ljubljana, Slovenia, September 2003.

[14] D. Middleton, "Statistical-physical models of electromagnetic interference," *IEEE Transactions on Electromagnetic Compatibility*, vol. 19, no. 3, part 1, pp. 106–127, 1977.

[15] D. Middleton, "Procedures for determining the parameters of the first-order canonical models of class A and class B electromagnetic interference," *IEEE Transactions on Electromagnetic Compatibility*, vol. 21, no. 3, pp. 190–208, 1979.

[16] M. Ghosh, "Analysis of the effect of impulse noise on multicarrier and single carrier QAM systems," *IEEE Transactions on Communications*, vol. 44, no. 2, pp. 145–147, 1996.

[17] M. Zimmermann and K. Dostert, "Analysis and modeling of impulsive noise in broad-band power line communications," *IEEE Transactions on Electromagnetic Compatibility*, vol. 44, no. 1, pp. 249–258, 2002.

[18] N. Suljanović, A. Mujčić, M. Zajc, and J. F. Tasič, "Computation of high-frequency and time characteristics of corona noise on HV power line," *IEEE Transactions on Power Delivery*, vol. 20, no. 1, pp. 71–79, 2005.

[19] P. Burrascano, S. Cristina, and M. D'Amore, "Performance evaluation of digital signal transmission channels on coronating power lines," in *Proceedings of IEEE International Symposium on Circuits and Systems (ISCAS '88)*, vol. 1, pp. 365–368, Espoo, Finland, June 1988.

[20] P. Burrascano, S. Cristina, and M. D'Amore, "Digital generator of corona noise on power line carrier channels," *IEEE Transactions on Power Delivery*, vol. 3, no. 3, pp. 850–856, 1988.

[21] J. H. Lodge and M. L. Moher, "Maximum likelihood sequence estimation of CPM signals transmitted over Rayleigh flat-fading channels," *IEEE Transactions on Communications*, vol. 38, no. 6, pp. 787–794, 1990.

[22] D. Makrakis, P. T. Mathiopoulos, and D. P. Bouras, "Optimal decoding of coded PSK and QAM signals in correlated fast fading channels and AWGN: a combined envelope, multiple differential and coherent detection approach," *IEEE Transactions on Communications*, vol. 42, no. 1, pp. 63–75, 1994.

[23] X. Yu and S. Pasupathy, "Innovations-based MLSE for Rayleigh fading channels," *IEEE Transactions on Communications*, vol. 43, no. 2–4, pp. 1534–1544, 1995.

[24] G. M. Vitetta and D. P. Taylor, "Maximum likelihood decoding of uncoded and coded PSK signal sequences transmitted over Rayleigh flat-fading channels," *IEEE Transactions on Communications*, vol. 43, no. 11, pp. 2750–2758, 1995.

[25] E. Eleftheriou and W. Hirt, "Improving performance of PRML/EPRML through noise prediction," *IEEE Transactions on Magnetics*, vol. 32, no. 5, part 1, pp. 3968–3970, 1996.

[26] M. V. Eyuboglu and S. U. H. Qureshi, "Reduced-state sequence estimation with set partitioning and decision feedback," *IEEE Transactions on Communications*, vol. 36, no. 1, pp. 13–20, 1988.

[27] A. Duel-Hallen and C. Heegard, "Delayed decision-feedback sequence estimation," *IEEE Transactions on Communications*, vol. 37, no. 5, pp. 428–436, 1989.

[28] P. R. Chevillat and E. Eleftheriou, "Decoding of trellis-encoded signals in the presence of intersymbol interference and noise," *IEEE Transactions on Communications*, vol. 37, no. 7, pp. 669–676, 1989.

[29] R. Raheli, A. Polydoros, and C.-K. Tzou, "Per-survivor processing: a general approach to MLSE in uncertain environments," *IEEE Transactions on Communications*, vol. 43, no. 2–4, pp. 354–364, 1995.

[30] G. Ferrari, G. Colavolpe, and R. Raheli, *Detection Algorithms for Wireless Communications, with Applications to Wired and Storage Systems*, John Wiley & Sons, London, UK, 2004.

[31] R. Pighi and R. Raheli, "Linear predictive detection for power line communications impaired by colored noise," in *Proceedings of IEEE International Symposium on Power Line Communications and Its Applications (ISPLC '06)*, pp. 337–342, Orlando, Fla, USA, March 2006.

[32] L.-F. Wei, "Trellis-coded modulation with multidimensional constellations," *IEEE Transactions on Information Theory*, vol. 33, no. 4, pp. 483–501, 1987.

[33] M. K. Simon, S. M. Hinedi, and W. C. Lindsey, *Digital Communication Techniques: Signal Design and Detection*, Prentice Hall-PTR, Englewood Cliffs, NJ, USA, 1994.

[34] G. Ungerboeck, "Channel coding with multilevel/phase signals," *IEEE Transactions on Information Theory*, vol. 28, no. 1, pp. 55–67, 1982.

[35] G. Ferrari, G. Colavolpe, and R. Raheli, "A unified framework for finite-memory detection," *IEEE Journal on Selected Areas in Communications*, vol. 23, no. 9, pp. 1697–1706, 2005.

[36] S. Haykin, *Adaptive Filter Theory*, Prentice-Hall, Englewood Cliffs, NJ, USA, 4th edition, 2001.

[37] H. Philipps, "Performance measurements of power line channels at high frequencies," in *Proceedings of the International Symposium on Power-Line Communications and Its Applications (ISPLC '98)*, pp. 229–237, Tokyo, Japan, March 1998.

[38] A. A. Smith Jr., "Power line noise survey," *IEEE Transactions on Electromagnetic Compatibility*, vol. 14, no. 1, pp. 31–32, 1972.

[39] T. Esmailian, F. R. Kschischang, and P. G. Gulak, "Characteristics of in-building power lines at high frequencies and their channel capacity," in *Proceedings of the International Symposium on Power-Line Communications and Its Applications (ISPLC '00)*, pp. 52–59, Limerick, Ireland, April 2000.

[40] M. Katayama, T. Yamazato, and H. Okada, "A mathematical model of noise in narrowband power line communication systems," *IEEE Journal on Selected Areas in Communications*, vol. 24, no. 7, pp. 1267–1276, 2006.

[41] P. S. Maruvada, *Corona Performance on High-Voltage Transmission Lines*, Research Studies Press, Baldock, UK, 2000.

[42] N. Suljanović, A. Mujčić, M. Zajc, and J. F. Tasič, "Corona noise characteristics in high voltage PLC channel," in *Proceedings of the IEEE International Conference on Industrial Technology (ICIT '03)*, vol. 2, pp. 1036–1039, Maribor, Slovenia, December 2003.

[43] S. Cristina and M. D'Amore, "Analytical method for calculating corona noise on HVAC power line carrier communication channels," *IEEE Transactions on Power Apparatus and Systems*, vol. 104, no. 5, pp. 1017–1024, 1985.

[44] P. Burrascano, S. Cristina, and M. D'Amore, "Digital generator of corona noise on power line carrier channels," in *IEEE Power Systems Conference and Exposition (PSCE '87)*, San Francisco, Calif, USA, July 1987.

[45] J. P. Burg, "Maximum entropy spectral analysis," in *Proceedings of the 37th Meeting of the Society of Exploration Geophysicists*, pp. 34–41, Oklahoma City, Okla, USA, 1967.

**Riccardo Pighi** was born in Piacenza, Italy, in November 1976. He received his Dr.-Ing. degree (Laurea) in telecommunication engineering and his Ph.D. degree in information technology from the University of Parma, Parma, Italy, in 2002 and 2006, respectively. He currently holds a postdoctorate position at the University of Parma. Since 2003, he has been involved in the project of a multicarrier system for power line communication (PLC) in collaboration with Selta S.p.A., Cadeo (PC), Italy. His main research interests are in the area of digital communication system design, adaptive and multirate signal processing, storage systems, information theory, and power line communications.

**Riccardo Raheli** received the Dr.-Ing. degree (Laurea) in electrical engineering (summa cum laude) from the University of Pisa, Italy, in 1983, the M.S. degree in electrical and computer engineering from the University of Massachusetts, Amherst, Mass, USA, in 1986, and the Ph.D. degree (Perfezionamento) in electrical engineering (summa cum laude) from the Scuola Superiore S. Anna, Pisa, Italy, in 1987. From 1986 to 1988, he was with Siemens Telecomunicazioni, Milan, Italy. From 1988 to 1991, he was a Research Professor at the Scuola Superiore S. Anna, Pisa, Italy. In 1990, he was a Visiting Assistant Professor at the University of Southern California, Los Angeles, USA. Since 1991, he has been with the University of Parma, Italy, where he is currently a Professor of communications engineering. He served on the Editorial Board of the IEEE Transactions on Communications as an Editor for Detection, Equalization, and Coding from 1999 to 2003. He also served as a Guest Editor of the IEEE Journal on Selected Areas in Communications, Special Issue on Differential and Noncoherent Wireless Communications, published in September 2005. Since 2003, he has been on the Editorial Board of the European Transactions on Telecommunications as an Editor for Communication Theory.